UNCLASSIFIED

AD 445004

DEFENSE DOCUMENTATION CENTER

FOR

SCIENTIFIC AND TECHNICAL INFORMATION

CAMERON STATION, ALEXANDRIA, VIRGINIA

UNCLASSIFIED

445004

D D C

AUG 3 1 1964

DDC-IRA   D

Yearly Progress Report No. 6
ELECTRON SPIN ECHO RESONANCE

Contract NOnr 2541 (00)
Project NR 048-125

3-53-64-2   June 1964

Electronic Sciences Laboratory
LOCKHEED MISSILES & SPACE COMPANY
A Group Division of Lockheed Aircraft Corporation
Palo Alto, California

Précis

<u>Title</u>: Yearly Progress Report No. 6, "Electron Spin Echo Resonance," M. A. Fischler and D. E. Kaplan, July 1964; Contract NOnr 2541(00), Project NR 048-125.

<u>Background</u>: The Electronic Sciences Laboratory of the Lockheed Missiles & Space Company is studying the application of microwave spin echo phenomena for use as a microwave pulse delay line in such areas as high-speed computer memories and advanced radar systems. With the method of electron spin echo resonance, pulsed microwave signals can be serially stored and recalled at an arbitrary later time within the relaxation time of the spin system.

<u>Condensed Report Contents</u>: The zero-field paramagnetic resonance spectra of weak crystalline field sites of cerium and praseodymium in calcium fluoride are presented with tentative conclusions regarding the symmetry of these sites. Preliminary relaxation time data on cerium doped calcium oxide are given. Considerations attendant to the utilization of helical slow wave structures for microwave spin echo experiments are discussed. A new proposal for a computer associative memory utilizing spin echo devices is given.

<u>For Further Information</u>: The complete report is available in the major Navy technical libraries and can be obtained from the Defense Documentation Center. A few copies are available for distribution by the authors.

FOREWORD

This document covers work done on the Electron Spin Echo
Resonance project by the Electronic Sciences Laboratory
of Lockheed Missiles & Space Company. This project is
conducted under contract to the Information Systems Branch
of the Office of Naval Research, Contract NOnr 2541(00),
Project NR 048-125.

Dr. M. A. Fischler and Dr. D. E. Kaplan contributed to
this report.

ABSTRACT

The zero-field paramagnetic resonance spectra of weak crystalline field sites of cerium and praseodymium in calcium fluoride are presented with tentative conclusions regarding the symmetry of these sites. Preliminary relaxation time data on cerium doped calcium oxide are given. Considerations attendant to the utilization of helical slow wave structures for microwave spin echo experiments are discussed. A new proposal for a computer associative memory utilizing spin echo devices is given.

CONTENTS

ILLUSTRATIONS

Section 1

INTRODUCTION

During this past year, research on this program has been directed toward implementing possible applications of electron spin echo phenomena. The primary objectives in the experimental work on paramagnetic materials have been to find systems that will support microwave spin echo phenomena in the absence of an external magnetic field and to find systems with long spin phase memory times. The utilization of slow wave structures, particularly helices, in place of resonant cavities to couple microwave power to the paramagnetic material has been studied. Slow wave structures afford substantial advantages over cavities with respect to driving power requirements, bandwidth, and output signal power. Theoretical considerations relating to the practical utilization of electron spin echo phenomena have been in progress in this interval and are discussed in Ref. 1.

In this progress report, experimental data of the past year are considered in some detail, including recent results that greatly enhance the application possibilities of spin echo phenomena. Some additional notes on the utilization of helices are presented and a new concept for utilizing a spin echo memory in a content addressable memory (CAM) system is discussed.

1

Section 2
MATERIAL STUDIES

The possible utilization of pure crystalline electric field interactions as a means for providing electron spin echo phenomena in the absence of an external magnetic field became a reality with the discovery of zero-field splittings at microwave X-band frequencies in cerium doped calcium fluoride (Ca , Ce)F_2. A preliminary report on this work was given at the August 1963 American Physical Society meeting (Ref. 2). Recently during this program exceedingly broad zero-field spectrum in praseodymium doped calcium fluoride (Ca , Pr)F_2 has been observed, also in microwave X-band. While the spectral properties of these materials are still being studied, it is possible to make some preliminary remarks regarding spectrum interpretation.

The calcium fluoride lattice is body-centered cubic with calcium ions occupying body centers of alternate cubes. Trivalent rare earth ions normally enter the lattice at Ca^{2+} sites. Charge compensation is effected by F^- ions entering the lattice at interstitial vacancies if the crystals are prepared in an inert atmosphere. Experimental evidence (Ref. 3) indicates that the charge compensating fluorine ions are only loosely bound to the rare earth and will migrate to the nearest neighbor interstitial positions only if the crystal is slowly annealed. Rapid quenching of a doped crystal may trap fluorine ions at sites quite distant from the paramagnetic impurity. In the latter case the local cubic field symmetry of the Ca^{2+} site is in principal preserved, while in the former case perturbations of the local charge distribution may result in tetragonal, trigonal, or orthorhombic fields, to mention the most common cases.

Some examples of possible paramagnetic sites are indicated in Fig. 1: (a) shows the normal CaF_2 lattice; (b) shows the common tegragonal site in annealed crystals, with a nearest neighbor F^- ion; (c) indicates a trigonal site due to an 0^{2-} ion replacing an adjacent fluorine ion — a fluorine ion in the next nearest neighbor position

2
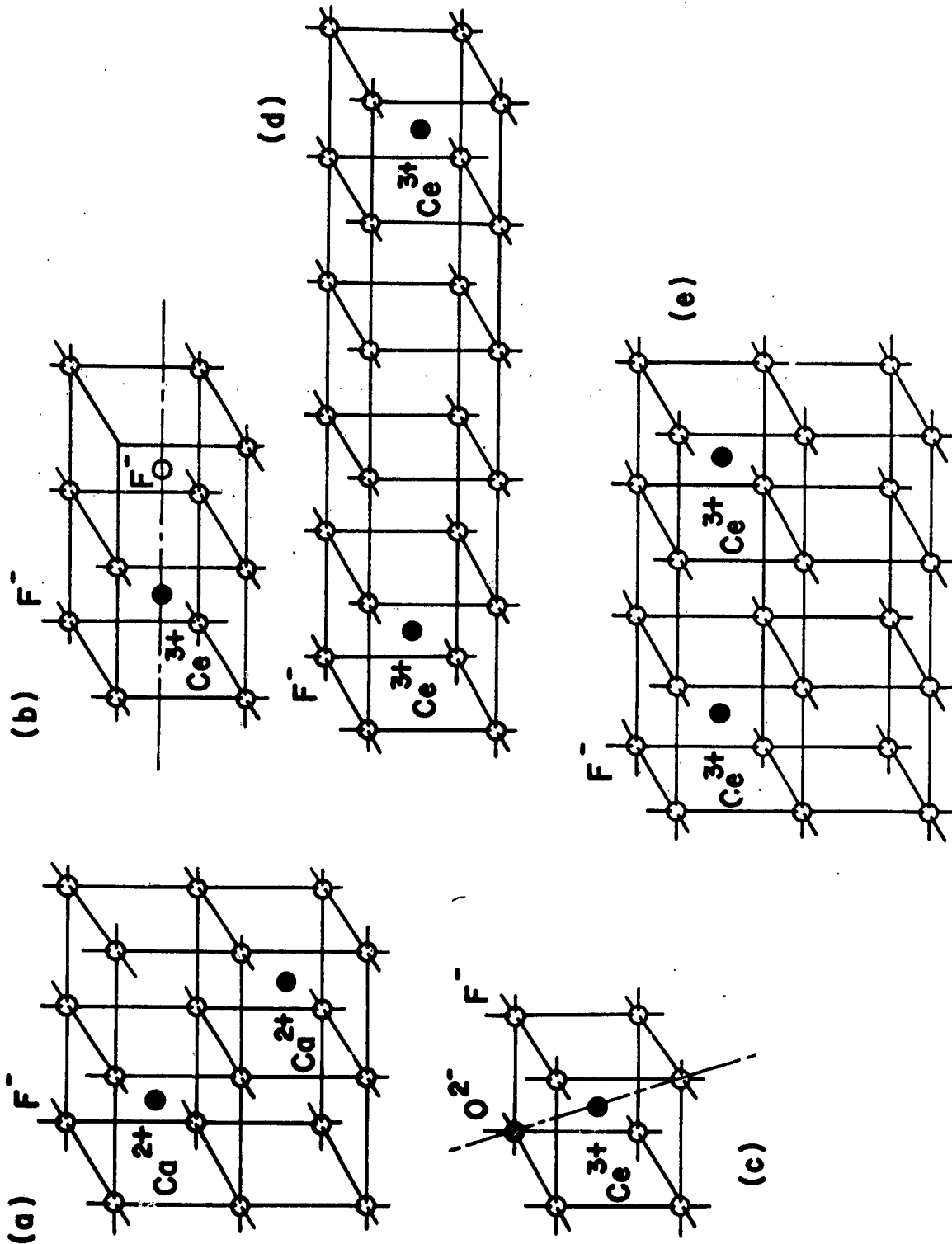
Fig. 1 Charge Compensation Sites for $(Ca, Ce)F_2$

3

also will create a trigonal field; (d) and (e) show weaker tetragonal perturbations arising from F^- or Ce^{3+} ions more removed along the cube axes.

While there have been numerous studies (Refs. 4, 5, 6) of the paramagnetic spectra and relaxation of rare earth ions in CaF_2, there remain major questions regarding the nature of the crystalline fields and the relaxation mechanisms in these materials. For example, the spin-lattice relaxation times for trivalent rare earth ions in CaF_2 exhibit a $1/T$ temperature dependence in the liquid helium temperature region suggestive of a direct relaxation process. The measured values of the relaxation times are, however, two to three orders of magnitude shorter than is expected on the basis of orbit-lattice coupling.

For the present in this program we are more concerned with certain anomalies in the paramagnetic spectra of the systems $(Ca, Ce)F_2$ and $(Ca, Pr)F_2$. $(Ca, Ce)F_2$ was one of the first of the rare earth dope fluorides that was studied but it does not now appear to be well understood. Early spectroscopy by Baker et al. (Ref. 4) identified a tetragonal site for Ce^{3+} due to a nearest neighbor F^- ion, but the assignation of the ground state wave functions in the tetragonal spectrum now appears uncertain. Weber's estimation of excited state separations on the order of 500 cm^{-1} are based on these data (Ref. 6). On the other hand, Dvir and Low (Ref. 5) have found a cubic site in a rapidly grown crystal, with evidence of a ground state Γ_8 quartet and an excited Γ_7 doublet removed approximately one wave number from the ground state. This ordering of levels is expected for the $^2F_{5/2}$ ground state in an eight-fold coordinated cubic field. However, this result has been questioned by subsequent investigators who have been unable to identify a cubic spectrum. Our own studies of the $(Ca, Ce)F_2$ system evidence the existence of a site with crystalline field splittings on the order of 0.3 cm^{-1}, with tentative indication that these splittings may be associated with cubic and near cubic spectra. While it is extremely difficult to reconcile such small splittings with evidence for much larger crystalline fields deduced from other resonance data for this system, there is sufficient uncertainty in all presently available data to justify an ad hoc interpretation of our results.

4

Few spectroscopic data on the system $(Ca, Pr)F_2$ have been reported. Neither Baker (Ref. 4) nor Low (Ref. 5) could observe paramagnetic resonance in 0.01 percent material. Weber (Ref. 6) has reported two weak isotropic lines in 0.6 percent material at $g = 2$, with widths of 20 and 100 gauss. In addition, he reports a broad intense line observable in low magnetic fields. Our own results indicate an exceedingly broad zero-field resonance covering a frequency range greater than 1.2 kMc in center X-band. We have not yet established limits on this resonance width. This result is compatible with Weber's low field observation.

The following description of experimental technique is presented because the method used in obtaining the data is novel. Paramagnetic spectroscopy is normally carried out at fixed frequency while amplitude modulating a linearly varying magnetic field. The primary reason for sweeping the magnetic field lies in the instrumental difficulty in varying, in a linear manner, klystron frequency and resonant cavity frequency while maintaining the klystron frequency coincident with that of the cavity. Some experimenters have attempted zero-field or fixed-field spectroscopy by other techniques, but with few exceptions there has been little activity in this area.

Use of spin echo phenomena for zero-field spectroscopy is a novel and powerful solution to the problem. Not only may the spin echo amplitude be utilized as an indicator of resonance absorption, i.e., a measure of M_z, but information permitting the identification of transitions between different spin states may be obtained from an examination of pulse power conditions for an effective $\frac{\pi}{2} - \frac{\pi}{2}$ pulse sequence, independently of signal amplitude. We note that matrix elements of the form $\langle j \mid J_\pm \mid j' \rangle$ appear in the argument of the function $\cos \gamma_e \langle \mid \rangle H_1 t_w$ which determines effective pulse angle in a spin echo experiment. If the pulse duration t_w is held constant and the electromagnetic coupling to the sample is independent of frequency, then comparison of the microwave power required to produce a $\frac{\pi}{2} - \frac{\pi}{2}$ pulse sequence for different transitions provides relative values of the respective matrix elements. Comparison of spin echo amplitudes, which are proportional to $\langle j \mid J_\pm \mid j' \rangle^2$, provides a cross check on these data for transitions associated with the same paramagnetic site. To trace out

5

the zero-field spectrum, it is then only necessary to measure spin echo amplitude as a function of frequency on a point-by-point basis. In practice, with short pulses of broad Fourier spectrum, a large frequency region can be mapped quickly.

Zero-field spectroscopic data have been obtained for $(Ca, Ce)F_2$ crystals of 0.1% Ce concentration, slowly annealed and quenched, at temperatures of 4.2° and 1.6° K. The annealed crystals show the two-line spectrum given in Fig. 2. The line at 9.365 kMc is approximately twice as intense as the line at 9.48 kMc. Relative microwave power values required to produce a $\frac{\pi}{2} - \frac{\pi}{2}$ pulse condition for the two lines are compatible, within the limits of experimental error, with the amplitude relationship for the two lines.

Data for the quenched material are shown in Fig. 3. The quenched crystal shows an intense line at 9.38 kMc and a spectrum of reduced intensity that appears to be identical to that observed in the annealed crystal. The dominant line in the quenched crystal is believed to be associated with a site of different symmetry from that appearing in the annealed spectrum.

We assume that a cubic site is favored in the quenched crystal and that there is a tendency in the annealing process for charge compensating fluorine ions to migrate toward the neighborhood of the cubic site, producing a distortion of the local cubic field. This distortion may be small in the case of fluorine ions more distantly removed than the nearest neighbor interstitial position. It is then tempting to assign the predominant single line in the quenched crystal spectrum to a pure cubic site, and the two line spectrum in the annealed case to a cubic field site subject to a slight perturbation in field that splits the Γ_8 quartet allowing two transitions to the Γ_7 doublet, which is unaffected in the presence of a lower order field component. The background spectrum for the quenched crystal presumably results from a small population of Ce^{3+} sites that have a relatively close neighbor F^- ion perturbing the field, as in the annealed material. Figure 4 shows the energy level scheme and wave functions for the $^2F_{5/2}$ ground state of the cerium ion in the presence of a cubic crystalline field (to the left

6
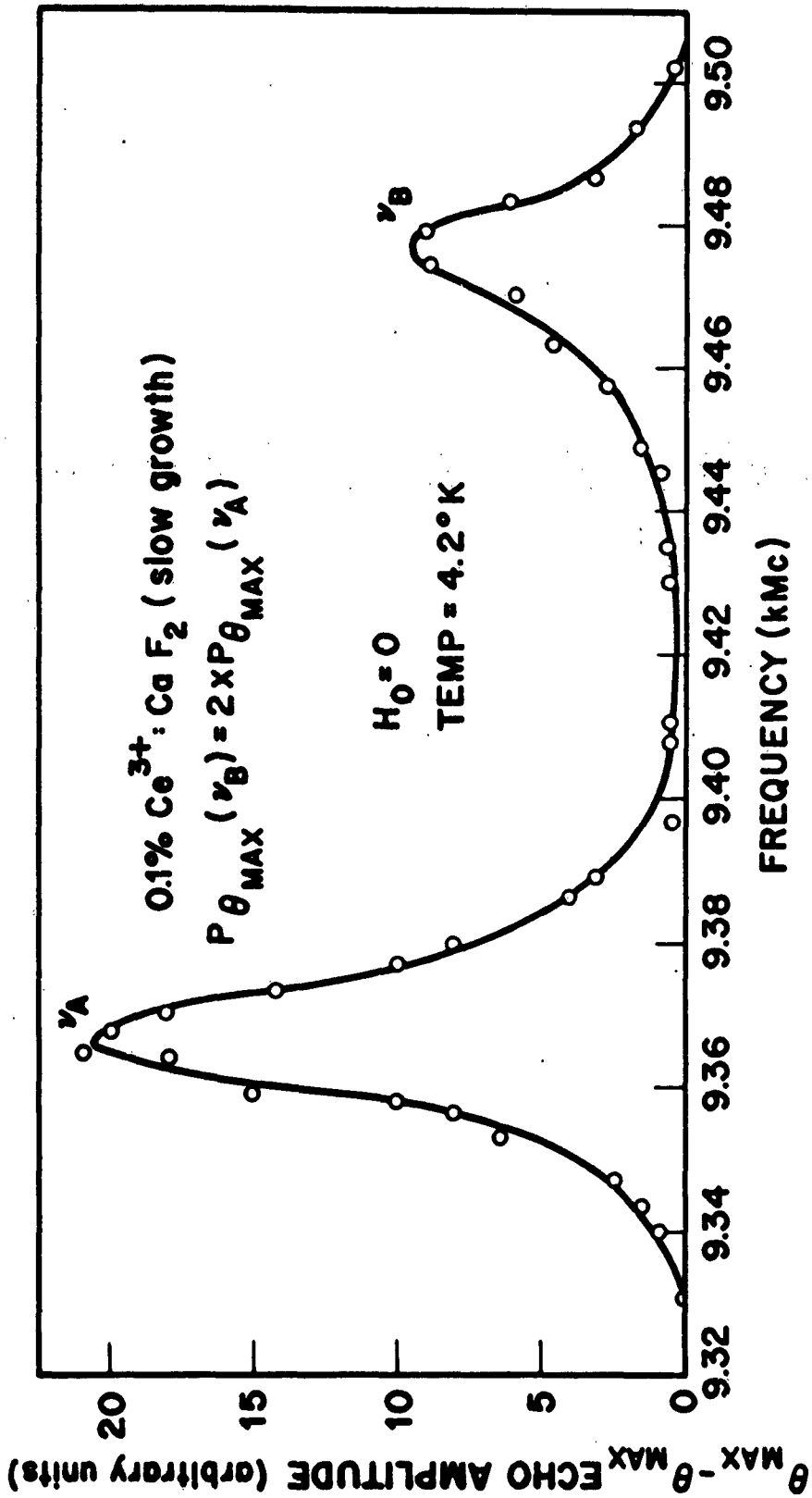
Fig. 2 Zero–Field Spectrum of Annealed (Ca , Ce)F$_2$

7
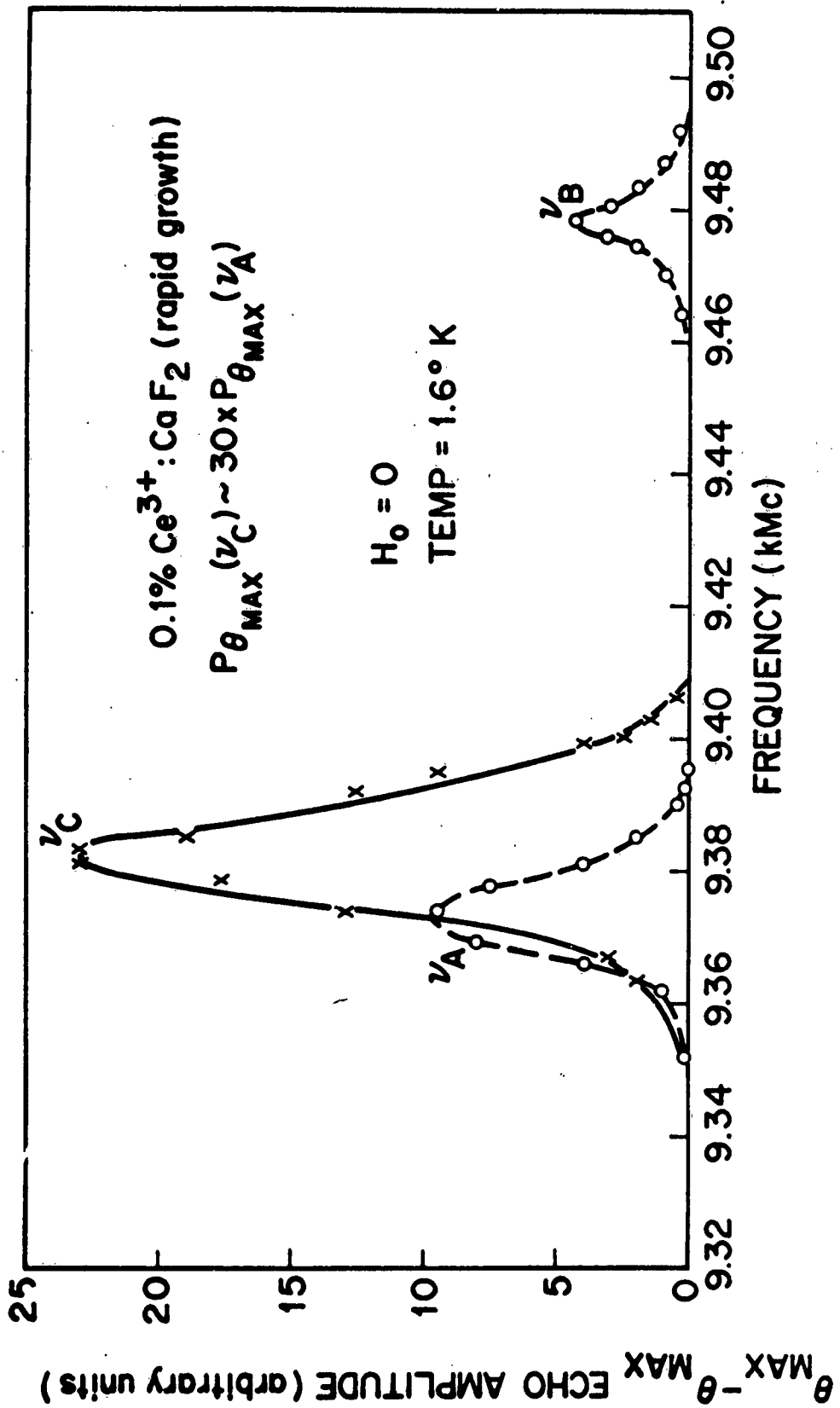
Fig. 3 Zero-Field Spectrum of Quenched $(Ca, Ce)F_2$

$(Ca,Ce)F_2$
Ce^{3+} $^2F_{5/2}$

AXIAL

CUBIC

$\sqrt{5/6}|3/2\rangle$
$-\sqrt{1/6}|5/2\rangle$

$-\sqrt{5/6}|-3/2\rangle$
$+\sqrt{1/6}|-5/2\rangle$

γ_A γ_B

$-|1/2\rangle + |-1/2\rangle$

$\sqrt{5/6}|5/2\rangle$
$\sqrt{1/6}|-3/2\rangle$

$\sqrt{5/6}|-5/2\rangle$
$-\sqrt{1/6}|3/2\rangle$

γ_C

Γ_7

Γ_8

$H \neq 0$

$H = 0$

$H = 0$

$H \neq 0$
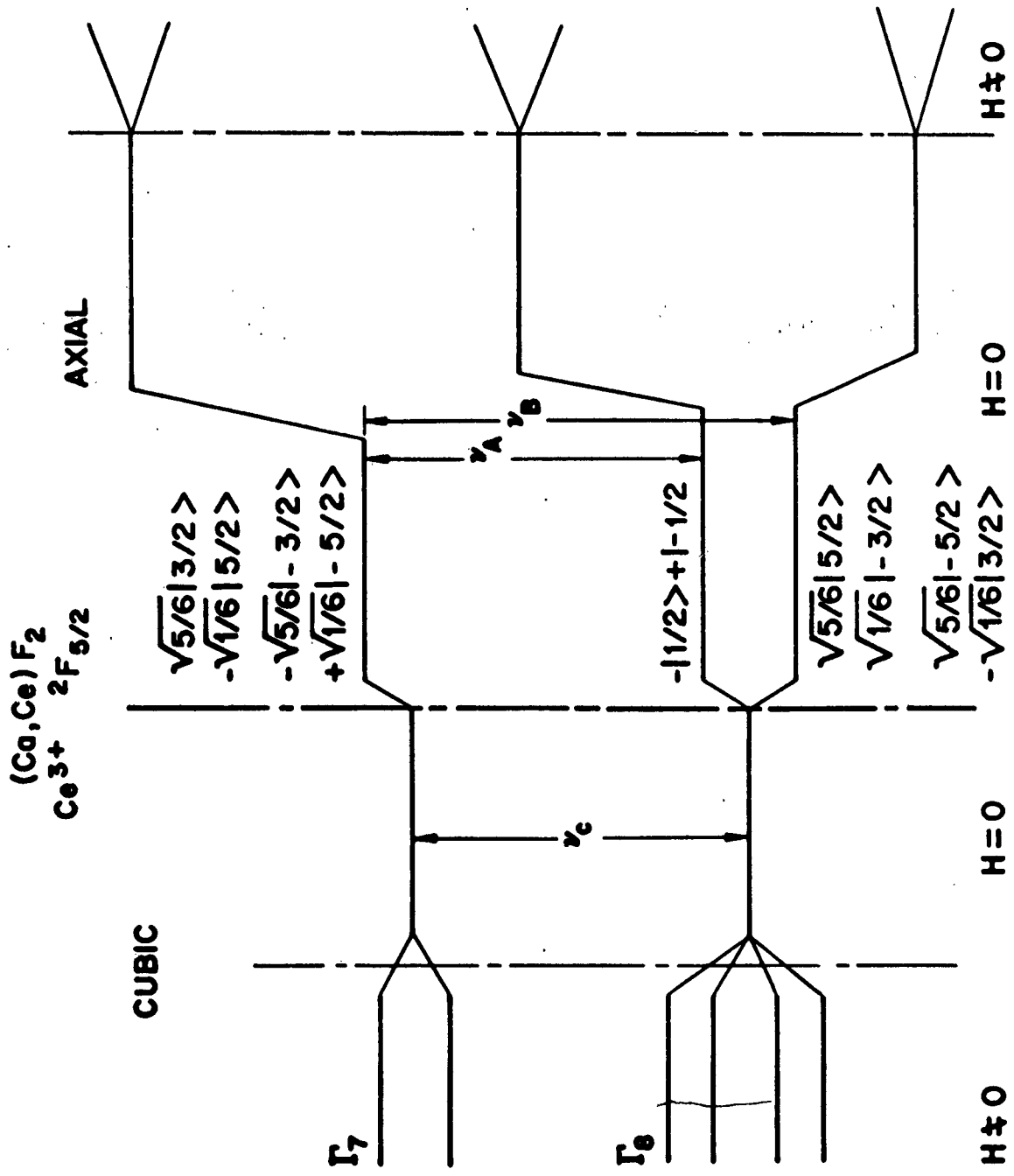
Fig. 4 Energy Level Splittings in $(Ca, Ce)F_2$

9

of the center line) and with the addition of a small lower order field perturbation (to the right of the center line).

Evaluation of the pulse power requirements for a $\frac{\pi}{2} - \frac{\pi}{2}$ pulse condition for the three lines on the basis of this model using wave functions, as given in Fig. 4, gives results considerably outside the limits of experimental error noted in Table 1.

Table 1

MICROWAVE POWER RATIO FOR $\frac{\pi}{2} - \frac{\pi}{2}$ PULSE CONDITION FOR $(Ca, Ce)F_2$
ZERO-FIELD SPECTRUM, WAVE FUNCTIONS AS GIVEN IN FIG. 4

Lines	Experimental Value (db)	Theoretical Value (db)
ν_A/ν_B	3	5
ν_A/ν_C	15	8

If, however, we assume slight admixing from the $J = 7/2$ state, which is not an unreasonable presumption, and adjust the mixing coefficient so that a good fit is obtained for the ν_A/ν_B ratio, we then find results as in Table 2.

Table 2

MICROWAVE POWER RATIO FOR $\frac{\pi}{2} - \frac{\pi}{2}$ PULSE CONDITION FOR $(Ca, Ce)F_2$
ZERO-FIELD SPECTRUM, ASSUMING FIRST EXCITED STATE WAVE
FUNCTIONS OF THE FORM $\mp | \pm 1/2 > \pm \alpha | \mp 7/2 >$, $\alpha \sim 0.18$

Lines	Experimental Value (db)	Theoretical Value (db)
ν_A/ν_B	3	3
ν_A/ν_C	15	13

A planned double resonance experiment should establish with certainty whether ν_A and ν_B are in fact associated with the same type of Ce^{3+} site and possibly lend credence to this model.

The limited results obtained for $(Ca, Pr)F_2$ at the time of this report are shown in Fig. 5, with a $(Ca, Ce)F_2$ annealed spectrum as a reference.
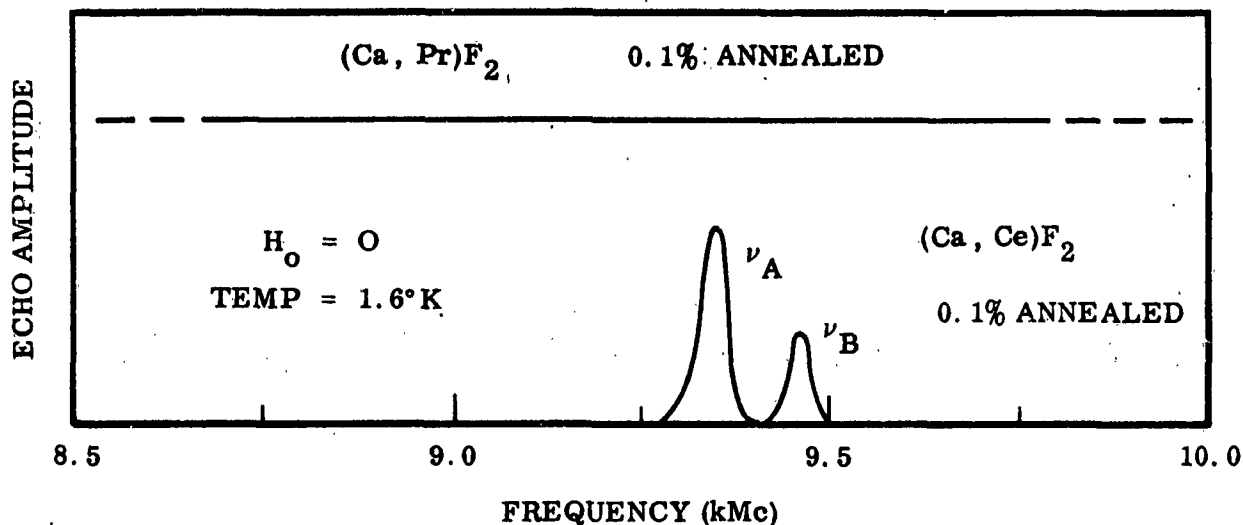
Fig. 5 Zero-Field Spectrum of $(Ca, Pr)F_2$

It is possible that this broad line is associated with a cubic site for the Pr^{3+} ion. If weak cubic fields in CaF_2 do indeed exist, a very broad zero field line could arise from transitions between the Γ_5 ground level of the $^3H_4$ state and the Γ_1, Γ_3, and Γ_4 excited levels for a certain range of ratios between the fourth and sixth degree coefficients of the cubic field. Reference is made here to Fig. 9 in the cubic field tabulation of Lea, Leask, and Wolf (Ref. 7), for x values in the vicinity of 0.85. An intensive analysis of this material is now in progress because of the application potential associated with the extremely broad zero-field linewidth.

Concomitantly, we have begun study of the spin echo properties of rare earth ions doped into calcium oxide CaO. There are two reasons for this choice. First, CaO is a lattice almost devoid of nuclear moment, the only contributions arising from 0.13% Ca^{43} and 0.03% O^{17}. A long spin phase memory time may be expected for

11

paramagnetic ions in an environment free of nuclear moment, provided that the ionic concentration is not high enough to cause appreciable spin-spin interaction. This is particularly true for ions with effective spin 1/2 as cross relaxation in multi-level systems may also shorten spin phase memory times. Second, the cubic fields in CaO are expected to be of roughly the same magnitude as those in CaF_2. The octahedral cubic coordination of CaO will generally cause level inversion with respect to the CaF_2 spectrum. However, if weak fields also exist in CaO, there is a possibility of accessible zero-field splittings in the microwave frequency region in this material. The possibility of obtaining materials with a zero-field spin echo response that also show phase memory times of hundreds of microseconds is singularly attractive.

Preparation of CaO crystals is extremely difficult because of the high reactivity and high melting point of this material. We have examined the Ce^{3+} phase memory time in the helium temperature region in poor quality experimental samples of (Ca, Ce)O. We have measured T_2's in excess of 100 μsec with usable storage times of 0.5 ms for inverse order storage. The T_1 of this material, which is presumably doped to about 0.01 % Ce^{3+} concentration, is about 10 sec, permitting z-axis storage for this length of time. Better quality samples of CaO doped with cerium and praseo-dymium have recently been obtained. Research on these materials is now in progress.

Section 3
SLOW WAVE STRUCTURES FOR ELECTRON SPIN ECHO EXPERIMENTS

The use of helical slow wave structures for paramagnetic resonance experiments has been considered in some detail by Webb (Ref. 8), and Siegman (Ref. 9) has discussed some generalized properties of slow wave structures for microwave resonance applications. A number of workers (Refs. 10, 11, 12) have utilized comb-type structures for traveling wave maser purposes. The properties of slow wave structures for electron spin echo purposes require special analysis because the conditions under which resonance is obtained are quite different from those in more conventional experiments. The unique advantages of helices over resonant cavities for electron spin echo experiments are pointed out in Ref. 1. It is shown there that for a helix of diameter such that only a fundamental axial mode is supported, there is approximately a 100-fold reduction in microwave power required to produce a given amplitude H_1 in the helix, as compared to a resonant cavity with a Q on the order of 100 at microwave X-band. There is also a concomitant 100-fold increase in signal from a given sample volume. Preliminary experiments have been conducted with X-band helices utilizing the organic free radical BDPA and $(Ca, Ce)F_2$ as paramagnetic samples. Results confirm the substantial advantages of helices for these experiments.†

Attention has been concentrated on helices because they are a relatively easy form of slow wave structure to fabricate and their electromagnetic properties can be formulated mathematically with convenience. They can be constructed with low dispersive properties, lending themselves particularly well to broadband operation, and are therefore attractive for possible applied uses of electron spin echo phenomena.

---

† A patent application has been filed on this aspect of this work.

There are certain practical problems associated with the utilization of helices in spin echo experiments.

- Coupling from a transmission line to a helix:

One primary requirement is to obtain a flat broadband match between the helix and transmission line. Since a similar problem exists in TWT technology, we have followed procedures used in that application. Two coupling methods that have been successfully employed are indicated schematically in Fig. 6. Figure 6a shows a transition in the form of a simple graduated pitch helix between a 50-ohm coaxial line and the sample helix. For appreciable bandwidths, at least five turns are required in the transition. The ground shell need not extend beyond the transition region since the fields external to the sample helix lie within a helix diameter of the surface.
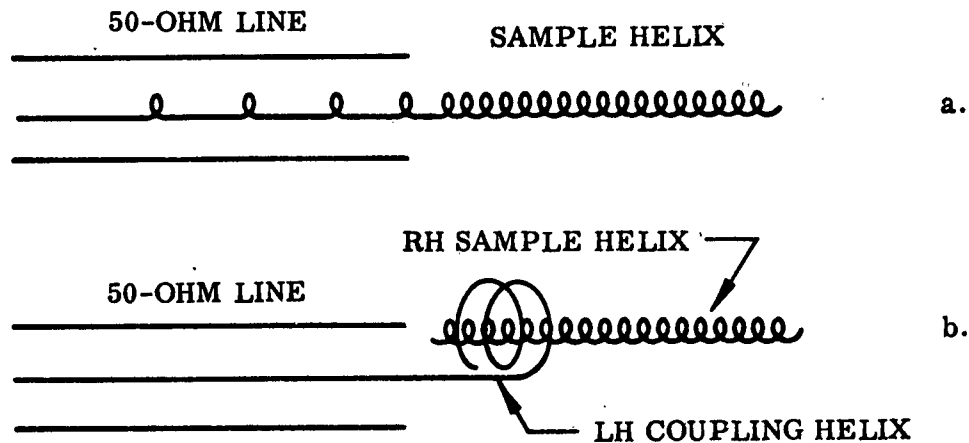
Fig. 6   Helix-Transmission Line Coupling Techniques

A second method capable of providing a good broadband match is the concentric coupler proposed by Cook et al. (Ref. 13). This is illustrated in Fig. 6b. The sample helix is surrounded by a larger diameter contrawound concentric helix, with diameter and turn ratio chosen so that the propagation velocities on both helices are equal when uncoupled. The outer helix, which is directly connected to the transmission line, need only be about one helix wavelength in length. It is found

14

that matching between the short outer helix and the transmission line presents no problem. The coupling and dispersive properties of this technique are critically dependent on the diameter ratio. We have obtained bandwidths on the order of 2 kMc with this type of coupler.

• Helix attenuation:

Because desirable sample volumes at microwave X-band frequencies are of the order of 1/20 to 1/5 cm^3, helix lengths of approximately 10 cm are necessary to contain the sample. This stems from the required restriction on helix diameter 2a and specific turn value n such that the condition $| \leq (4\pi^2 na^2/\lambda_o) \leq 1.5$ is satisfied. The helix then supports primarily only the fundamental axial electromagnetic mode. For n = 15 to 20, a diameter of approximately 1.5 mm is required. The paramagnetic element must not have excessive contact with the inner surface of the helix to minimize helix attenuation. A sample of square or triangular cross section is therefore indicated. A 1.5-mm diameter helix then must be approximately 10 cm in length to contain a square element of 0.1 cm^3 volume.

It was found initially that helices fabricated in the laboratory had attenuation factors on the order of 1 db/mm axial length. This is in agreement with Webb's values (Ref. 8) but is not in accord with theory. These values are intolerably high for use with 10-cm long helices. We have determined that helical substructures for low-power traveling wave tubes, modified to our specifications by eliminating the loss coating on the supporting rods and copper plating the molybdenum wire, show approximately 100 times less attenuation. We have successfully utilized such helices 8 cm in length for spin echo experiments and it now seems possible to fabricate suitable helices 10 cm in length with a total axial loss not exceeding 1 to 1.5 db. The reasons for this extreme reduction in loss in the commercially fabricated helices are not clearly understood but appear to be associated with the surface finish of the wire and the uniformity of the winding.

15

- Signal phasing problems:

The use of helices in electron spin echo experiments introduces special phasing problems that bear on signal amplitude. We note that the helix wavelength is $\lambda = 2\pi/\beta$ where β may be typically 30 cm^{-1} for a suitable X-band helix. X-band helix wavelengths are then on the order of 2 mm, while the lineal dimension of the sample might be 50 times this long. If a signal is introduced at one end of the helix, then the free precession signal generated by an element Cdz of the sample and appearing at the point of introduction will be characterized by an amplitude function which is given by

$$dA_1(t, z) = C\left[\exp(-j\omega t)\exp\left(-j\omega\frac{z}{v_g}\right)\exp\left(-j\omega\frac{z}{v_g}\right)\right]dz \quad , \quad A_1 = \int_0^\ell dA_2(z)$$

and at the opposite end by the function

$$dA_2(t, z) = C\left[\exp(j\omega t)\exp\left(-j\omega\frac{z}{v_g}\right)\exp\left(-j\omega\frac{\ell - z}{v_g}\right)\right]dz \quad , \quad A_2 = \int_0^\ell dA_2(z)$$

Notice has been taken of the phase of the signal emitted by the element Cdz. Performing the indicated integrations with respect to z, and assuming $v_g = v_p$ for these helices, the expression for the total signal appearing at the point of introduction is

$$A_1 = \frac{\exp(-j\omega t)}{j}\frac{C\lambda}{2\pi}\frac{-\exp\left(-j4\pi\frac{\ell}{\lambda}\right) + 1}{2}$$

and at the opposite end,

$$A_2 = \left[\exp(j\omega t)\exp\left(-j\frac{2\pi\ell}{\lambda}\right)\right]C\ell$$

16

Therefore, while the signal that appears at the opposite end is directly proportional to the volume of the sample $C\ell$, the maximum signal appearing at the point of introduction occurs for a sample length of an odd multiple of $\lambda/4$, and is then proportional to $C\lambda/2\pi$ regardless of the total sample length. This is because of phase interference effects in the backward wave for the coherently excited sample. Therefore, the signal A_2 is greater than the signal A_1 by a factor of $2\pi\ell/\lambda$. For an optimum X-band helix, this ratio is equal to about 300, corresponding to a difference of 40 db in power. It is therefore essential to recover the signal from the opposite end of the helix from the point of introduction.

MODIFIED ELECTRON SPIN ECHO SPECTROMETER SYSTEM

To facilitate variable frequency spectroscopy, the spin echo spectrometer has been modified in a manner that permits flexible operation in the frequency domain and provides a short pulse and complex code capability not previously available. The refined spectrometer system is shown schematically in Fig. 7. The principal change is the incorporation of a PPM 15 watt traveling wave tube and octave bandwidth X-band circulator in place of the relatively narrowband magnetron transmitter and narrowband circulator. The 15 watt power output of the TWT is adequate for experiments using reduced height cavities, and far more than is needed for use with most slow wave structures. A broadband solid state switch consisting of three varactor diodes in series before the TWT input is included to prevent cold leakage from the signal generator from creating noise at the receiver. The varactor switch is normally off and is gated on simultaneously with modulating pulses applied to the TWT grid. The entire system has modest modulation power requirements and is capable of generating 10 nsec pulses.

Measurements are taken as a function of frequency merely by retuning the local oscillator and resonant cavity to the appropriate frequency points. When a slow wave structure is utilized, only the local oscillator need be tuned.

18

MICROWAVE GENERATOR

BROADBAND DIODE SWITCH UNIT

TWT L-3472

SYSTEM CLOCK

PULSE CODE GENERATOR

OSCILLOSCOPE

SYNC

MICROWAVE STRUCTURE AND CRYOGENIC SYSTEM

VIDEO AMPLIFIER

SUPERHETERODYNE RECEIVER

GATE

LOCAL OSCILLATOR
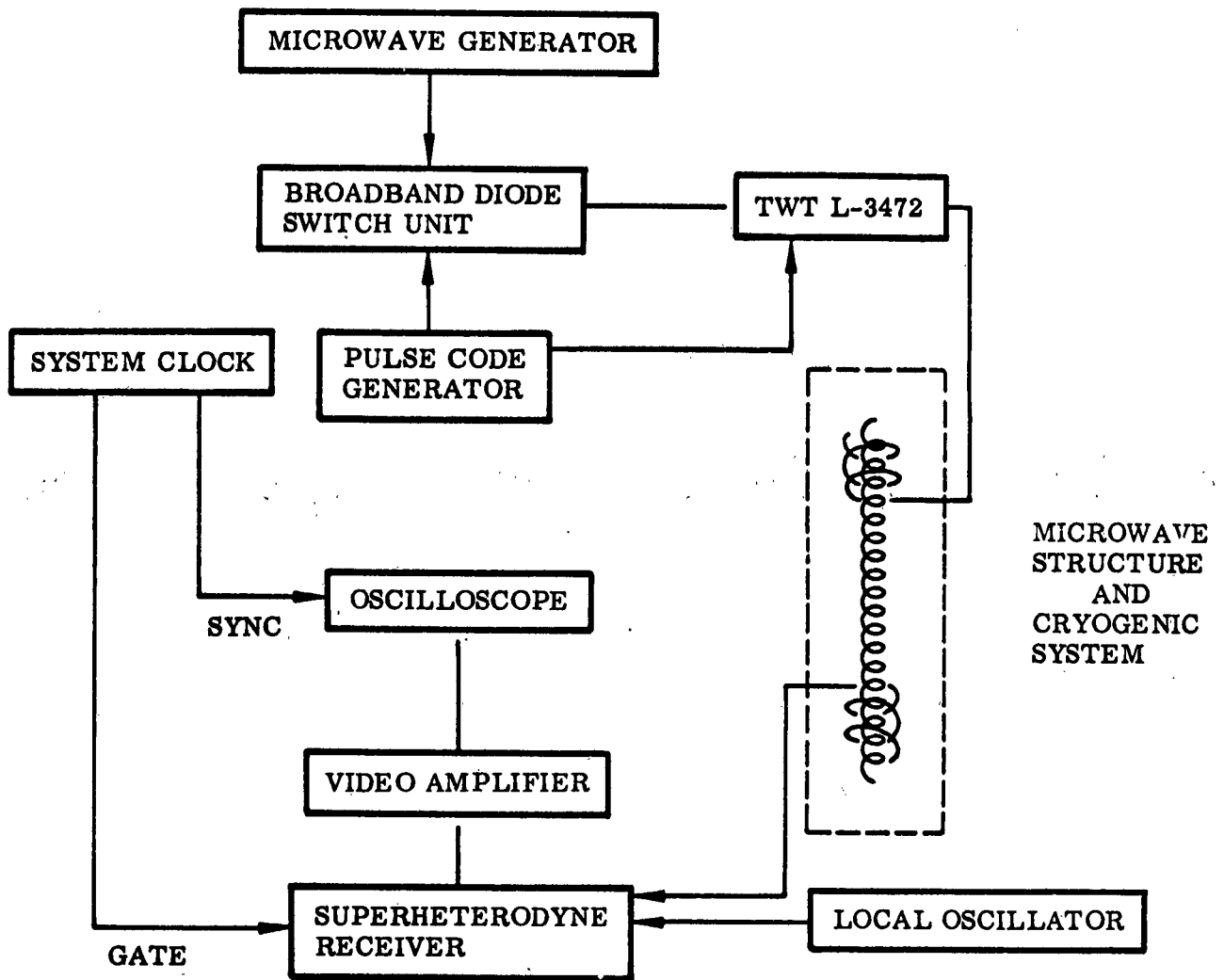
ALTERNATE RESONANT CAVITY SYSTEM

1

2

OCTAVE BANDWIDTH CIRCULATOR

RESONANT CAVITY

TWT OUTPUT

3

RECEIVER
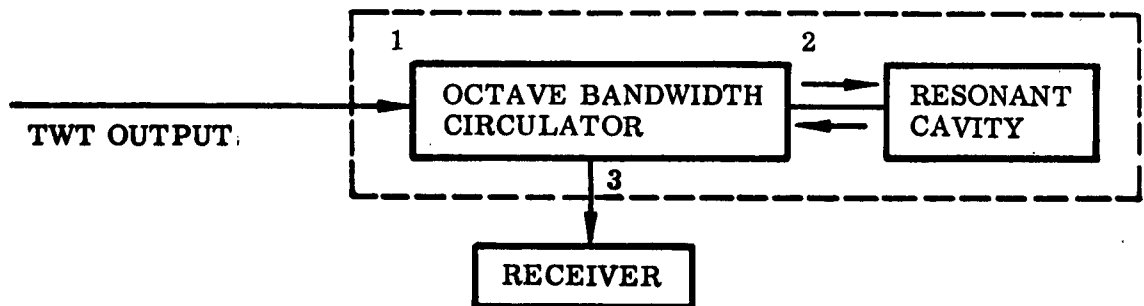
Fig. 7 Broadband Microwave Spin Echo Spectrometer System

19

Section 5
PROPOSAL FOR PROGRAMMABLE STORAGE UNIT EMPLOYING
SPIN ECHO MEMORY

INTRODUCTION

Several proposals for possible application of electron spin echo phenomena were considered in Ref. 1. Particular attention was given in that report to computer memory functions. This section presents a new proposal concerning a content addressable memory (CAM) based on electron spin echo devices. This proposal assumes an information processing rate of 100 Mc. Subsequent to the formulation of this proposal, it became evident that the spectral properties of $(Ca, Pr)F_2$ would permit, in principle, zero-field operation of a spin echo device at information processing rates in excess of 1.2 kMc, or alternatively, utilization of a single spin echo memory element for more than 10 channels, each 100 Mc wide. The estimates of cost and bit capacity which relate to previous work are now subject to substantial favorable revision in light of this new result. Bandwidth measurements on $(Ca, Pr)F_2$ are not complete at this time. The possibility exists that the full width for this system may in fact be substantially in excess of 1.2 kMc. Accordingly, we will defer estimates of memory system parameters and costs based on $(Ca, Pr)F_2$ until more data are available.

It should be mentioned that possibilities for utilization of spin echo phenomena as a microwave pulse command delay for radar ECM applications are also substantially enhanced by the existence of a broadband zero-field material of this kind.

It was previously suggested (Ref. 1) that a content addressable memory (CAM) system could be constructed, using spin echo memory (SEM) devices, which would be compatible with conventional computer system operating times. That is, most conventional computers have random access memory cycle times of from 2 to 10 μsec, flip-flop (ff)

20

registers that can operate at an information rate of from 5 to 10 Mc, and gates which have delay times of from 30 to 50 nsec. The suggested CAM would be an independent unit constructed with SEM devices, microwave hardware, and tunnel diode switches. Maximum access time for 512 words of storage would be 5.12 μsec at an estimated cost of 2 to 4 dollars per bit. This assumes that information is processed serially by word and parallelly by bit at a 100-Mc information rate.

Since more conventional techniques of constructing a CAM lead to prices of 5 to 15 dollars per bit, the prospects of a program to develop a SEM-CAM had seemed only marginal. There are some organizational concepts involving a SEM-CAM which make it a much more attractive device competitively as compared to a conventional CAM. These organizational concepts were obtained in connection with determining memory requirements for information retrieval systems, and thus have application here as well as for a memory which is an adjunct to a general-purpose computer. Figure 8 shows the central store organization in this system, and Fig. 9 shows the organization for one information channel.

Basically, the SEM permits us to construct a serial, programmable, very high information rate computer having an elementary command structure, and which would appear externally as a very versatile memory with the following properties:

- It could act as a CAM with a 5 μsec cycle time and thus be compatible with existing general-purpose memory systems. Search requests can specify varied logical relations between the bits of the stored data which must be satisfied for a match to be detected. This ability to do logical complex content addressing cannot be duplicated in any reasonable economic manner in a conventional CAM with comparable cycle times. Since the SEM-CAM uses serial techniques, the hardware logical structure does not have to be iterated as would be required in a parallel search system operating at a much lower basic information rate. In the SEM-CAM, the entire content of the memory effectively passes by a window once every 5 μsec.

21
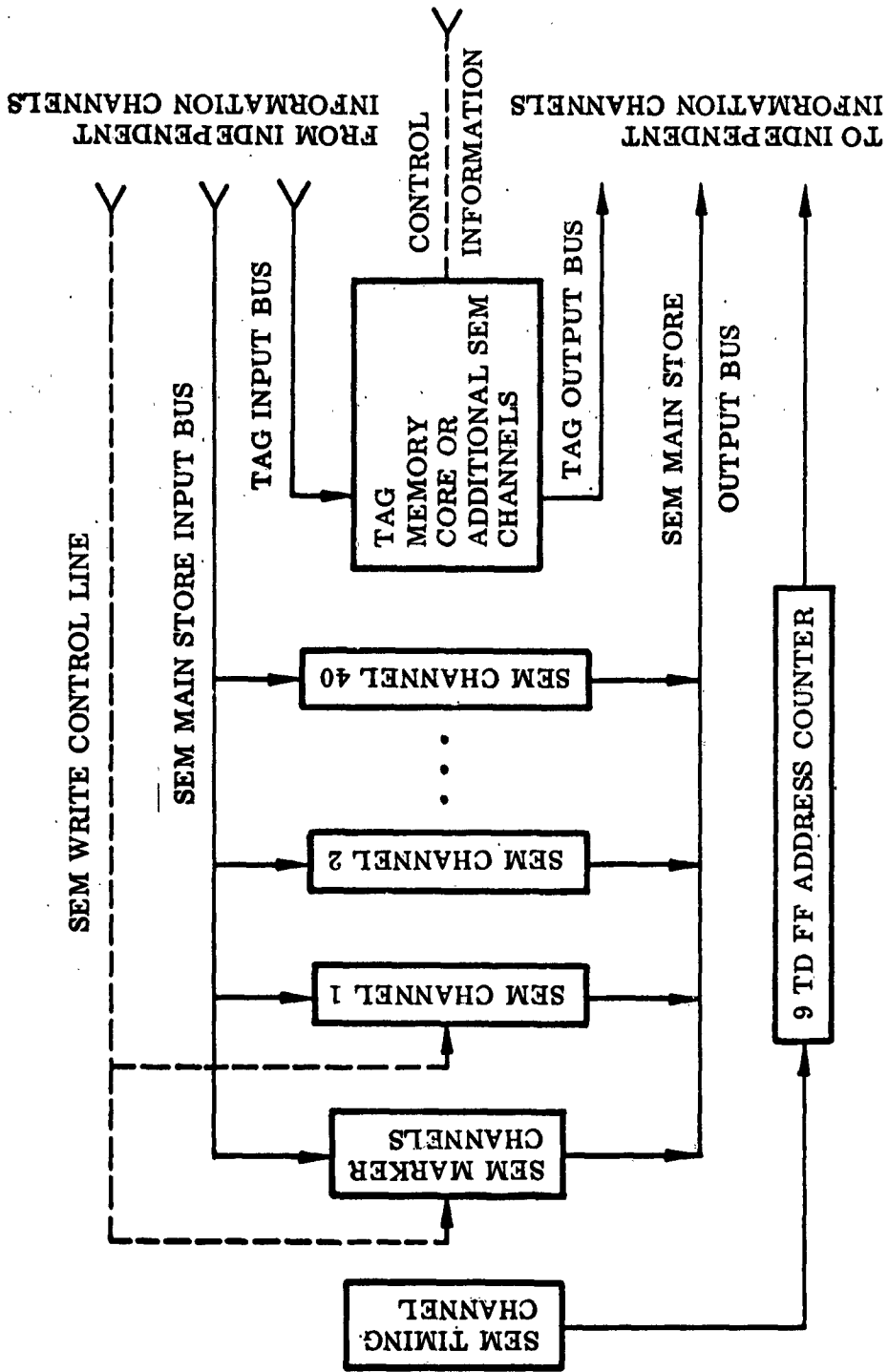
Fig. 8 SEM-CAM Central Store Organization

22

Fig. 9 SEM-CAM Information Channel Organization
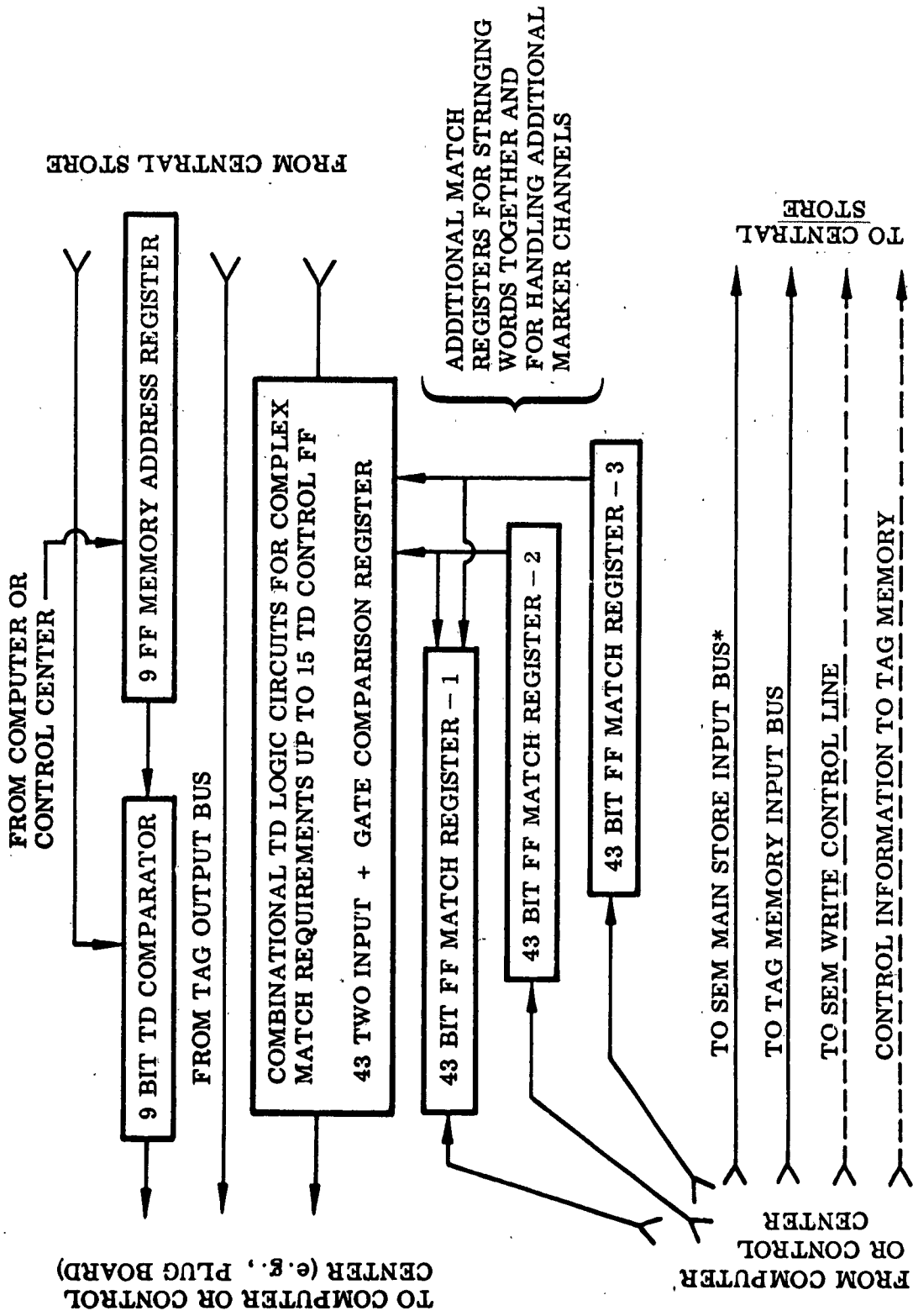
*Note: Some marker channels will be reserved for only one information channel

23

- The SEM-CAM can simultaneously and independently service a large number of data channels (limited only by cost considerations), providing a 2.5 μsec average access time for either random access or content addressing (content addressing at a higher cost for this mode of operation). This multiple port memory capability would be extremely useful in both multiprograming and multiprocessing operations (directory for relocating program segments) for table lookup, indexing, dictionary reference, and in a conventional computer organization for simultaneous computing and input-output operations. The multiple-port concept does not have a reasonably economic counterpart using conventional hardware.
- The SEM-CAM can easily string together words so that the entire data store appears to be one long connected string. This same operation can be accomplished in a conventional CAM, but again at greater cost.

ROUGH COST ESTIMATES

The unit costs used in the rough cost estimates are:

$1500 per SEM channel

$ 30 per conventional 10-Mc ff

$ 60 per tunnel diode ff

$ 40 per two-input tunnel diode exclusive-or gate

A complete information channel would cost (assuming none of the registers needed are available in the computer — an assumption which is very conservative):

3 43-bit registers = 43 $\times$ 30 $\times$ 3 $\approx$ $ 4,000	
150 tunnel diode logic gates	6,000
9-bit match address register	300
15 tunnel diode ff	900
Total $\approx$ $12,000	

A minimal information channel would involve:

1 43-bit register	≈ $1,200
60 tunnel diode logic gates	2,500
9-bit match address register	300
Total	≈ $4,000

One additional item not shown in the block diagram might be a 43-bit tunnel diode shift-register for string processing of data. This item would probably be associated with the main SEM store if required, and would cost approximately $5,000.

The cost of the main SEM store as shown (assuming three marker channels) is:

43 SEM channels	≈ $65,000
9 tunnel diode ff address counter	600
	≈ $65,600

An additional 5,000 to 10,000 dollars should be added for any system for packaging, power supplies, integration costs, etc.

TYPICAL SYSTEMS

Dictionary or Table Lookup

Memory is divided functionally into two subsystems — one stores the data and the other stores descriptive or tag data. Words (prefixes, suffixes, key words, descriptions, etc.) or arguments are loaded into the SEM store and are then left unaltered. The tags, definitions, labels (such as parts of speech), or functional values, are inserted in additional SEM channels or into a random access core store (say 2 μsec cycle time) so that the addresses of words in the SEM and corresponding addresses of definitions in the core are identical.

If English letters are coded in 5-bit cores, each word of the SEM store would correspond to an eight-letter English word. Since the dictionary here is limited to 500

25

entries, words of more than eight letters could probably be abbreviated to eight letters without ambiguity. Where more than one match is possible, this condition can be noted by a mark in a marker channel so that an additional look-up step can be taken.

Each information channel would require a minimum configuration and operation would be as follows. An item to be addressed from a given information channel is loaded into the single match register for that channel. The tunnel diode comparison register is set to detect a direct match, and the occurrence of a match will be detected at the time the data are dumped onto the output bus. If the tag memory is also SEM, the tag is dumped at the same time as the item in question, and is simultaneously available to all information channels. However, if the tag memory is core, the address counter will contain the core memory address of the required tag (or definition) and this address can be immediately interrogated for the required information if only one information channel is operating. If multiple information channels are used with the core store, then a queuing problem will be encountered at the core, and will have to be resolved by additional control logic. The economics of the situation appear to favor using additional SEM channels for multiple channel operation and a core store for single channel operation.

This dictionary or table lookup system could be used as follows:

- Parts of speech determination: In the computer programing procedure developed at LMSC, the main SEM memory contains prefixes, suffixes, and roots; and the tag memory contains parts of speech. Multiple channels could be operating on same or different documents.
- Indexing of document: The main SEM memory contains key words, descriptors, or uniterms. The tag memory contains indexing code symbols, the weighting to be assigned to the descriptor (for weighted indexing system), address for storing number of occurrences of that descriptor in document, etc. If desired, instead of reading information out of the tag memory, the tag memory can be used to store the occurrence count for the corresponding keyword or descriptor. After the document has been scanned (by entering its contents, one word at a time, into the match

26

register), the tag memory can be searched in the content addressable mode (assuming it is a SEM store) to locate all key words which occurred more than some predetermined number of times. These words can now be assigned as index terms to the document.

File Indexing

The descriptor sets for items in a file are inserted in the match register one at a time. For this application, say only 20 bits of the match register are used, each bit position indicates the relevance or irrelevance of a descriptor to the document. The main SEM store would contain search requests composed of a 20-bit descriptor vector and 20 control bits to specify the logical relations desired among the bits of the descriptor vector for a match. The control bits can be used to set up the tunnel diode combinatorial match logic. The tag memory would contain the address or identification of the search requestor, and on a match condition, the accession number of the document (whose storage is not shown in the block diagram) is routed to the appropriate requestor.

As a final comment, it should be noted that while all hardware references here were made to the SEM, the storage and processing techniques are equally applicable to other serial storage media if similar relative speed/cost attributes can be obtained.

27

Section 6
REFERENCES

1. Lockheed Missiles & Space Company, Tech. Rept. No. 4, NOnr 2541(00), Project NR 048-125, 3-53-64-1, Sunnyvale, Calif., Jun 1964

2. D. E. Kaplan, Bull. Am. Phys. Soc., Ser. II, Vol. 8, 1963, p. 468

3. E. Friedman and W. Low, J. Chem. Phys., Vol. 33, 1960, p. 1275

4. J. M. Baker, W. Hayes, and D. A. Jones, Proc. Phys. Soc., Vol. 73, 1959, p. 136

5. M. Dvir and W. Low, Proc. Phys. Soc., Vol. 75, 1960, p. 136

6. M. J. Weber and R. W. Bierig, Raytheon Technical Memorandum T-520, 1963; R. Bierig, M. Weber, and S. Warshaw, Raytheon Technical Memorandum T-521, 1963 (These references provide an excellent guide to the literature on paramagnetic spectroscopy of rare earth ions in calcium fluoride)

7. K. R. Lea, M. J. M. Leask, and W. P. Wolf, J. Phys. Chem. Solids, Vol. 23, 1962, p. 138

8. R. H. Webb, Rev. Sci. Inst., Vol. 33, 1962, p. 732

9. A. E. Siegman, Tech. Rept. No. 155-3, Signal Corp Contract DA36(039)SC-73178

10. R. W. DeGrosse, E. O. Schulz-DuBois, and H. E. D. Scovil, Bell System Tech. J., Vol. 38, 1959, p. 305

11. W. S. C. Chang, J. Cromack, and A. E. Siegman, 1959 IRE WESCON Conv. Rec., Part 1, 1959, p. 142

12. H. D. Tenney, R. W. Roberts, and P. H. Vartanian, 1959 IRE WESCON Conv. Rec., Part 1, 1959, p. 151

13. J. S. Cook, R. Kompfner, and C. F. Quate, Bell System Tech. J., Vol. 35, 1956, p. 127

Technical Library
Director Defense Res. & Eng
Room 3C-128, The Pentagon
Washington, D. C. 20301

Defense Documentation Center   20 cc.
Cameron Station
Alexandria,Virginia 22314

Chief of Naval Research   2 cc.
Department of the Navy
Washington 25, D. C.
Attn Code 437, Information Systems Branch

Director, Naval Research Laboratory   6 cc.
Technical Information Officer/Code 2000/
Washington 25, D. C.

Commanding Officer, Office of Naval Research   10 cc.
Navy #100, Fleet Post Office Box 39
New York, New York, 09599

Commanding Officer
ONR Branch Office
207 West 24th Street
New York 11, New York

Office of Naval Research Branch Office
495 Summer Street
Boston, Massachusetts 02110

Naval Ordnance Laboratory
White Oaks
Silver Spring 19, Maryland
Attn Technical Library

David Taylor Model Basin
Code 042 Technical Library
Washington D. C. 20007

Naval Electronics Laboratory
San Diego 52, California
Attn Technical Library

Dr. Daniel Alpert, Director
Coordinated Science Laboratory
University of Illinois
Urbana, Illinois

Air Force Cambridge Research Labs
Laurence C. Hanscom Field
Bedford, Massachusetts
Attn Research Library, CRMXL-R

U. S. Naval Weapons Laboratory
Dahlgren, Virginia 22448
Attn G. H. Gleissner/Code K-4/
Asst Director for Computation

National Bureau of Standards
Data Processing Systems Division
Room 239, Bldg. 10
Attn A. K. Similow
Wash 25, D. C.

George C. Francis
Computing Lab, BRL
Aberdeen Proving Ground, Maryland

Office of Naval Research
Branch Office Chicago
230 N. Michigan Avenue
Chicago, Illinois 60601

Commanding Officer
ONR Branch Office
1030 E. Green Street
Pasadena, California

Commanding Officer
ONR Branch Office
1000 Geary Street
San Francisco 9, California

Stanford University
Stanford, California
Attn Electronics Lab.,
Prof. John G. Linvill

National Physical Laboratory
Teddington, Middlesex
England
Attn Dr. A. M Uttley, Superintendent,
Autonomics Division

Commanding Officer
Harry Diamond Laboratories
Attn Library
Washington, D. C. 20438

Commanding Officer and Director
U. S. Naval Training Device Center
Port Washington
Long Island, New York
Attn Technical Library

Department of the Army
Office of the Chief of Research & Development
Pentagon, Room 3D442
Washington 25, D. C.
Attn Mr. L. H. Geiger

National Security Agency
Fort George G. Meade, Maryland
Attn Librarian. C-332

Lincoln Laboratory
Massachusetts Institute of Technology
Lexington 73, Massachusetts
Attn Library

Daniel E. Kaplan
Dept. 52-40, Bldg. 202
Lockheed Missiles and Space Company
3251 Hanover Street
Palo Alto, California